Advances in Science and Technology Research Journal

Advances in Science and Technology Research Journal 2022, 16(6), 14–22
https://doi.org/10.12913/22998624/155055
ISSN 2299–8624, License CC-BY 4.0

Received: 2022.08.18
Accepted: 2022.11.17
Published: 2022.12.01

The Influence of Normal Pressure on the Friction Force Reduction Effect Caused by Longitudinal Tangential Vibrations

Mariusz Leus[1*], Marta Rybkiewicz[1], Marcin Woźniak[1]

[1] Faculty of Mechanical Engineering and Mechatronics, West Pomeranian University of Technology in Szczecin, al. Piastów 19, 70-310 Szczecin, Poland

* Corresponding author's email: mariusz.leus@zut.edu.pl

ABSTRACT

The article presents the results of experimental research and numerical analysis of the effect of normal pressures on the level of friction reduction caused by longitudinal tangential vibrations. The experimental characteristics of tangential compliance of steel-steel junction with specific roughness as a function of surface pressure are presented. The simulation tests were performed in the Matlab/Simulink environment. Dynamic friction models were used in the calculations i.e., the Dahl model and the elasto-plastic model. These models consider both the tangential compliance of contact and the phenomenon of presliding displacement. The experimental tests were carried out on a specially made test stand. Root Mean Square Error (RMSE) was used to assess the compatibility of the results of numerical calculations with the results of experimental tests. It has been shown that the change of normal pressures has a significant impact both on the level of friction force reduction and the contact stiffness. For higher normal pressures, a better agreement with the experimental data is achieved by the elasto-plastic model.

Keywords: reduction of friction force, longitudinal tangential vibrations, stiffness of contact.

INTRODUCTION

In the mechanical systems, it is often necessary to minimize the force required to start sliding motion and the force that maintains this movement. For this reason, numerous studies are carried out to develop methods to reduce frictional resistance during the slid of one body after another. The own research [1÷5] and the works of other authors [6÷13] indicate that introducing the ground, on which the movement take place, into the vibrating motion in the direction of the tangent to the direction of slid can reduce the drive force F_d. This phenomenon is identified with the reduction of average friction force $\bar{F}_f$.

The level of force reduction depends on many factors and can vary dramatically. It depends both on the vibrating parameters such as frequency f and amplitude u_o, and on the motion parameters – drive velocity v_d. The tangential stiffness of the contact zone between the ground and the moving body also has a significant impact on the reduction level. The value of this stiffness depends on parameters such as normal pressures, frictional pair materials or the roughness of the contact surfaces.

In this work, the Dahl model [14, 15] and the elasto-plastic model [16, 17] were used for the numerical analysis of the effect of longitudinal tangential vibrations on the friction force. In the adopted models, the friction force is a function of the contact tangential stiffness, which is described by coefficient k_t. Therefore, numerical analyzes with the use of these models require the adoption of correct, i.e., real value of this coefficient. Assuming the incorrect value of k_t leads to an incorrect determination of the level of the friction force reduction. The value of this coefficient is determined experimentally based on the compliance characteristics plotted in the tangential direction for a given contact joint. Examples of such studies are presented in [18÷21].

The tests of contact joints are also carried out in the normal direction to the contact surface [18, 22]. The compliance characteristic

determined in this direction are important for the modeling process of the normal vibrations effect on the friction force [23, 24], or in the case of modeling of elements joined in multi-bolted connections [25, 26]. The introduction of the normal contact stiffness characteristic to the multi-bolted connection model allows for a better description of the behavior of this connection compared to the modeling traditionally used in commercial FEM programs, in which it is only possible to specify the normal contact stiffness coefficient constant in time.

The previous experimental and numerical studies of the influence of longitudinal tangential vibrations on the friction force carried out by the authors of this paper were mainly carried out with the set normal pressures p and the changing vibration parameters, i.e., amplitude u_o and frequency f. Therefore, the purpose of this study was to analyze the friction force reduction as a function of normal pressures p at the set values of u_o and f. The experimental tests were carried out for steel-steel friction pair with a defined roughness of the contact surfaces. The obtained results were compared with the results of simulation tests carried out with the use of abovementioned dynamic friction models. The values of the tangential stiffness coefficient for the tested sliding pair were also experimentally determined as a function of normal pressures, the knowledge of which is necessary for performing numerical analyzes based on the adopted friction models. It has been shown that the adoption of an elasto-plastic friction model in the procedures of numerical analysis of the effect of longitudinal tangential vibrations on the friction force can significantly improve the accuracy of predicting the level of friction force reduction, especially for higher normal pressures.

EXPERIENTAL RESEARCH

Experimental research on the friction force reduction

The purpose of the experimental research was to determine the influence of normal pressures p on the achieved level of the friction force reduction in the presence of longitudinal tangential vibrations. The tests were carried out on test stand which was described in detail in [1]. The view of the mechanical part of the test stand with the control, recording and signal processing apparatus is shown in Figure 1. The main part of this stand is a sliding pair composed of a specially designed upper sample (1) and lower sample (2). Both samples are made of steel C45 and their nominal contact area is 1200 mm^2. The upper sample is moved by a special driver (7) at a certain velocity v_d. The lower sample is attached to the table (3)

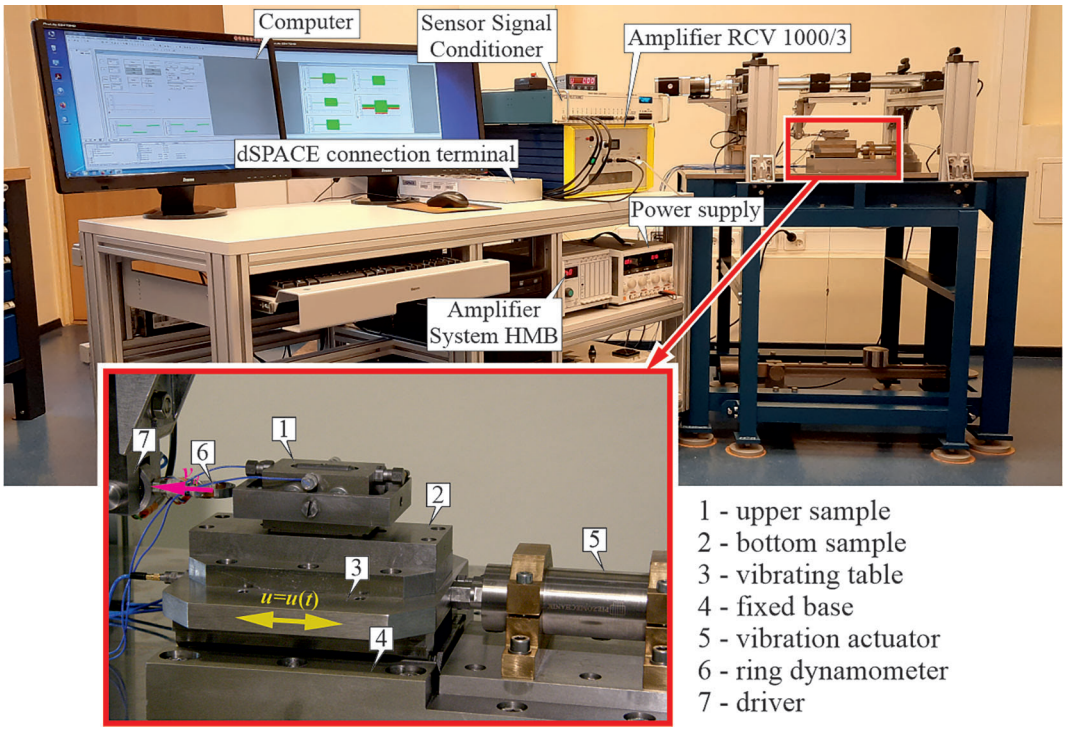

Fig. 1. The view of the test stand

placed on roller guides and on which vibrations can be forced by a piezoelectric indicator (5). The given mechanical system rests on a stationary base (4). The drive force F_d is measured by a ring dynamometer located between the driver and the upper sample. Storck et al. [11] indicates that the driving force F_d is equals the average friction force $\bar{F}_f$ over one period of vibration T in most systems with the friction force reduction effect caused by longitudinal tangential vibrations. Hence it can be assumed that $F_d \approx \bar{F}_f$.

The experimental tests were carried out for the steel-steel dry contact. The roughness factor R_a of the contact surface of the lower sample was R_a = 1.35 µm, and that of the upper sample R_a = 0.44 µm. In each series of tests, the vibration frequency f and amplitude u_o as well as the drive velocity v_d were constant. The value of normal surface pressures p was changed in the range form p_{min} = 0.014 N/mm² to p_{max} = 0.112 N/mm². The experimental research was conducted with the harmonic excitation of frequency f = 2000 Hz and amplitude u_o = 0.1 µm for four values of the drive velocity, i.e.: 0.2, 0.5, 1 and 2 mm/s.

Figure 2 presents examples of time characteristics of the drive force F_d measured in two successive stages of the upper sample movement. These characteristics were determined at the drive velocity v_d = 0.5 mm/s for three values of normal pressures p equal to: 0.095, 0.063 and 0.030 N/mm². In the first stage, the sliding movement of upper sample was carried out without base vibrations and in the second stage – at the forced vibrations.

Summary plot presents the dependence of friction force reduction coefficient $\rho = \bar{F}_f / F_C$ as a function of normal pressures p. This diagram was made based on a set of experimental time characteristics of drive force F_d. In the sliding motion on the vibrating base the average value of friction force $\bar{F}_f$ is equal to measured drive force F_d. In a slip without vibrations, the friction force is equal to the Coulomb friction force F_C. The value ρ = 1 means no reduction of the friction force, while when ρ < 1 the reduction takes place. The smaller value of this coefficient, the greater the reduction of the friction force.

The parameter having a significant impact on the level of friction force reduction in sliding motion in the presence of longitudinal tangential vibrations is the ratio of drive velocity v_d to the amplitude of vibration velocity $v_a = u_o 2\pi f$. A necessary condition for the reduction of the friction force with this type of vibration is that $v_a > v_d$, which has been confirmed in many research studies [1÷13]. When this condition is not satisfied, the reduction of the friction force does not occur. In the presented experimental tests for the assumed amplitude of vibration u_o = 0.1 µm, the amplitude of vibration velocity was v_a = 1.26 mm/s. Thus, it is greater than the first three assumed drive velocity v_d = 0.2, 0.5 and 1 mm/s. The presented plot shows that for these drive velocities in the entire range of normal pressures p, the friction force in the sliding motion is reduced due to the introduction of longitudinal tangential velocities. The obtained results indicate that the change of normal pressures can reduce the effectiveness of this reduction in certain intervals. This is clearly visible for v_d = 0.5 and 0.2 mm/s. For the last of the assumed velocity values v_d = 2 mm/s, i.e. the variant when $v_a < v_d$, the coefficient ρ remains at the constant level ($\rho \approx 1$). Thus, in this case, there is no reduction in the friction force in the entire range of the analyzed values of normal pressures p.

Experimental tests of contact compliance

Correct numerical analysis with the use of dynamic friction models requires the determination of the actual value of the contact stiffness

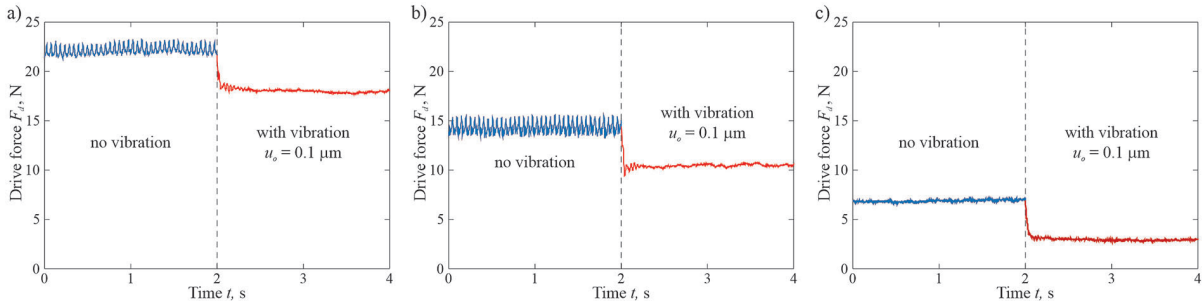

Fig. 2. Experimental time characteristics of the drive force for dry contact of steel-steel: a) p = 0.095 N/mm², b) p = 0.063 N/mm², c) p = 0.030 N/mm²

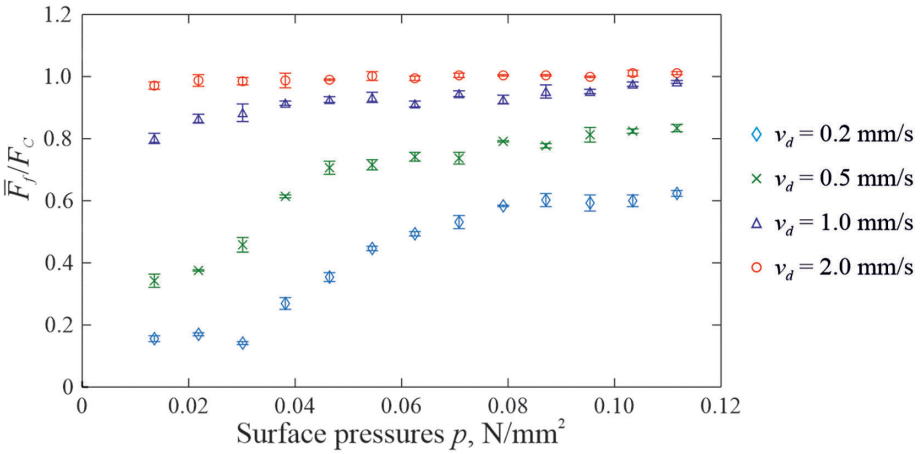

Fig. 3. The dependence of friction force reduction coefficient $\rho = \bar{F}_f/F_C$ as a function of normal pressures p

coefficient k_t. The value of this coefficient can be obtained from experimental characteristics of the contact compliance. In the order to determine it, the tangential stiffness of contact was tested. These experimental tests were carried out for the steel-steel contact with the same surface roughness and normal pressures as assumed as in the previous experimental tests of friction force reduction in the presence of longitudinal tangential vibrations. Figure 4 shows the load diagram of the tested contact and the obtained compliance characteristics determined in the tangential direction with the smooth increase of the tangential load F_t from zero to the assumed maximum value. The change of the normal pressures p was implemented by additional external loads F_z. These characteristics were determined on a special test sand described in [21]. Based on the obtained characteristics, the values of the coefficient k_t were determined. Figure 5 presents a plot of the dependence of this coefficient on normal pressures p.

The presented results (Fig. 4 and Fig. 5) confirm the clear dependance of the contact tangential stiffness on the normal pressure p. The increase in the value of this parameter causes a gradual increase in the value of the tangential stiffness coefficient k_t at the given values R_a of the contact area.

COMPUTATIONAL MODEL

Fundamental mathematical relationships

Numerical analysis were carried out on the model described in detail in [2], which is used to study the effect of longitudinal tangential vibrations on the friction force. As in the experiment in the model is assumed that the upper body of mass m is moved by the drive on the base (Fig. 6a), which can be set into vibration movement at any time. The direction of forced vibrations is parallel

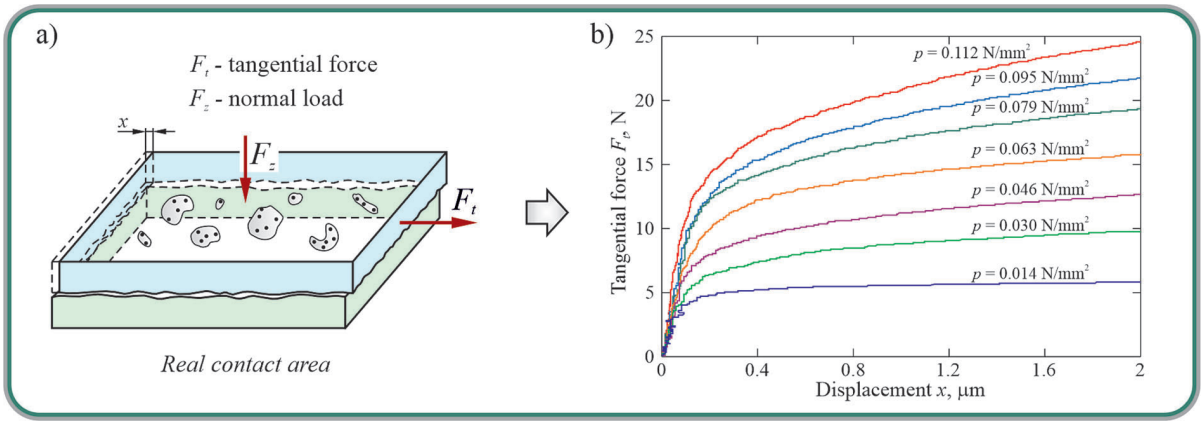

Fig. 4. Flat contact joint: a) the diagram of load implementation, b) the compliance characteristics of steel-steel contact for various pressures p

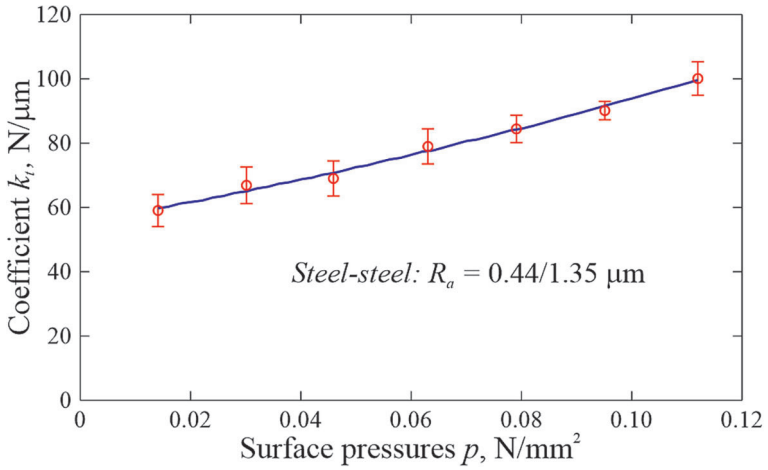

Fig. 5. Dependence of the stiffness coefficient k_t on normal pressures p

to the direction of slip. The contact zone (Fig. 6b) is a deformable and can be modeled with micro springs (Fig. 6c), which deform under tangential load in the direction of friction force F_f. Finally, the system of micro springs is reduced to one bar element *MN* with the tangential stiffness coefficient k_t. The point of application of the drive force F_d moves in the direction of this force with the pre-set drive velocity v_d.

The motion equation of the upper sample, sliding in the direction of the drive force F_d has the following form:

$$m\ddot{x} = F_d - F_f \tag{1}$$

The drive force F_d occurring in the above equation can be determined from the dependence:

$$F_d = k_d(s_d - x) \tag{2}$$

where: k_d – stiffness coefficient of the drive system,
x – displacement of the moving body,
s_d – displacement of the drive force starting point:

$$s_d = v_d t \tag{3}$$

where: v_d – drive velocity,
t – time.

The method of friction force F_f determining depends on the adopted friction model. In the both the analyzed friction models, i.e., the Dahl model [14, 15] and the elasto-plastic model [16, 17], the friction force is determined from a simple relationship:

$$F_f = k_t s \tag{4}$$

where: k_t – tangential stiffness coefficient of contact,
s – elastic deformation of the contact in the tangential direction.

The s component is related to the elastic deformation of the contact surface unevenness in the direction of the friction force F_f (Fig. 6d). The rate of change this component value in these friction models is a function of both the contact stiffness k_t and the relative velocity v_r of the sliding body and the ground.

$$\frac{ds}{dt} = v_r\left[1 - \beta(s, v_r)\frac{k_t}{F_C}sgn(v_r)s\right]^{\alpha} \tag{5}$$

F_C is the Coulomb friction force:

$$F_C = \mu F_N \tag{6}$$

where: μ – static friction coefficient,
F_N – normal reaction of the ground.

The exponent of the power α in the equation (6) in both adopted friction models for elasto-plastic materials is equal to 1 [27]. In the case of Dahl model, also the function describing the tangential displacement in successive phases is equal to 1. It results from the assumption that in given model, the deformations of contact are elasto-plastic from the initial stage of loads and can be represented in two components – elastic s

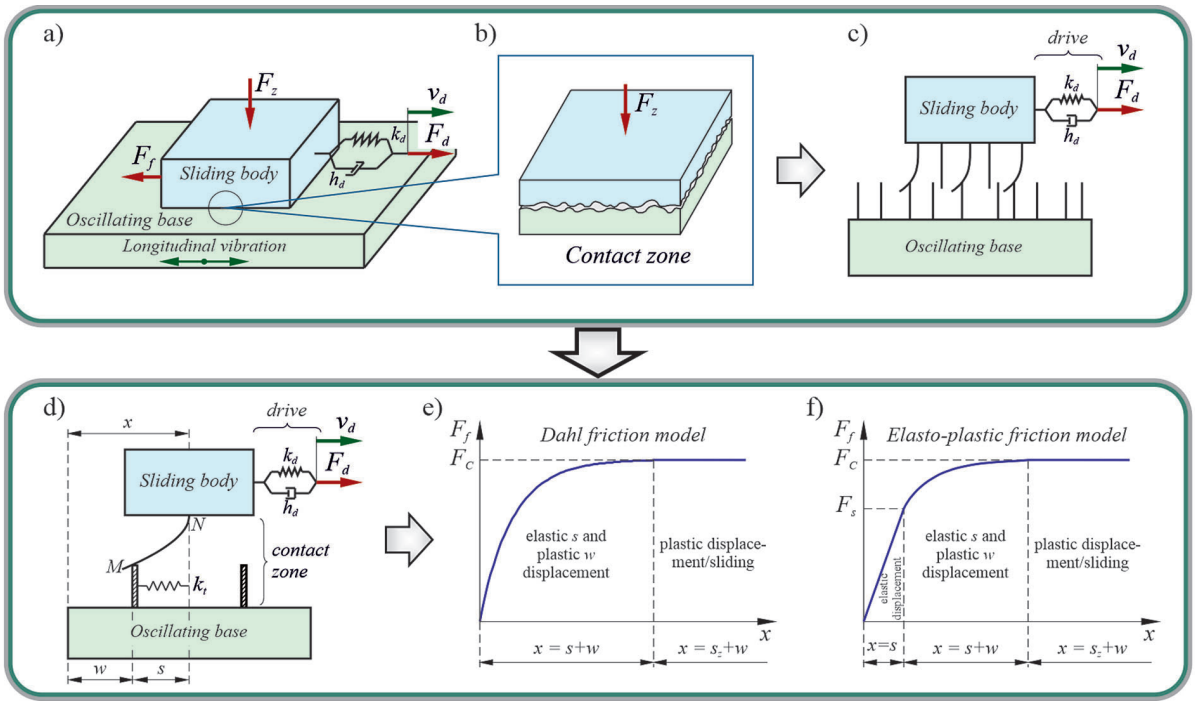

Fig. 6. Contact zone modeling: a) the sliding pair, b) the real contact zone, c, d) the stages of modeling roughness protrusions, e, f) the compliance characteristics for dynamic friction models

and plastic w (Fig. 6d). When the elastic component of this deformation reaches the limit value $s_z = F_C/k_t$, the macroscopic contact breaks and the sliding movement of the sliding body begins. In the elasto-plastic models, Dupont et al. [16, 17] added purely elastic deformation phase for the initial displacement (Fig. 6f). This phase continues until the component s reaches the value of s_s (where: $s_s = 0.7s_z$). Then there is an elasto-plastic deformation phase $s_s < s < s_z$ and, as a result, the slide phase $(s_s = s_z)$. The function proposed by Dupont et al. [16, 17] has the form:

$$\beta(s, v_r) = \begin{Bmatrix} 0 & for & |s| \le s_s \\ \beta_m(s) & for & s_s < |s| < s_z \\ 1 & for & |s| \ge s_z \end{Bmatrix} \quad when \quad sgn(v_r) = sgn(s) \quad (7)$$
$$and \qquad \beta(s, v_r) = 0 \qquad when \quad sgn(v_r) \neq sgn(s),$$

where:

$$\beta_m(s) = \frac{1}{2} sin\left(\pi \frac{s - \frac{1}{2}(s_z + s_s)}{s_z - s_s}\right) + \frac{1}{2} \quad (8)$$

In the calculations, as in the experimental tests, it was assumed that the ground vibrating motion is harmonic and can be described by the relationship:

$$u = u_o \, sin(\omega t) \quad (9)$$

hence the vibration velocity:

$$\dot{u} = v_a \, cos(\omega t) \quad (10)$$

where: u_o – vibration amplitude,
v_a – vibration velocity amplitude,
ω – angular frequency of vibrations $(\omega = 2\pi f)$,
f – vibrations frequency.

The symbol v_r in (5) denotes the relative velocity of the upper body in sliding motion relative to the vibrating ground

$$v_r = \dot{x} - \dot{u} \quad (11)$$

Computational procedures in Matlab/Simulink

Based on the above mathematical relationships, a computational algorithm was developed in the Matlab/Simulink environment to analyze the impact of the ground longitudinal tangential vibrations on the level of friction force reduction in sliding motion. Figure 7 presents a diagram of the developed algorithm using the Dahl friction model and the elasto-plastic model.

In the presented algorithm, the developed numerical procedures have been grouped into four

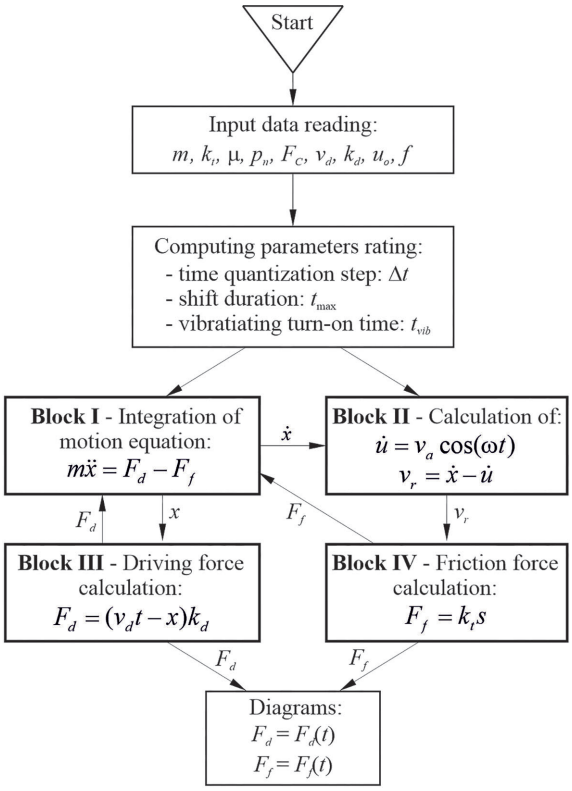

Fig. 7. Algorithm for calculating the friction force in sliding motion at longitudinal vibrations

main calculation blocks. Each of these blocks is responsible for a different stage of calculation:

- Block I – Integration block of the motion equation of the sliding body along the axis *0x*. This module determines the acceleration $\ddot{x}(t)$, the velocity $\dot{x}(t)$ and the displacement $x(t)$ of body being moved.
- Block II – Block of the velocities $\dot{u}$ and v_r. This module determines the ground vibrations velocity $\dot{u}(t)$ and the relative velocity $v_r(t)$.
- Block III – Block of the drive force. This module determines the value of the drive force F_d.
- Block IV – Block of friction force. This module determines the value of friction force F_f.

SIMULATION STUDIES

The results of the experimental tests were compared with the results of simulation test carried out with the use of computational procedures described above. As already mentioned, these procedures used dynamic friction models i.e., the Dahl model and the elasto-plastic model. The calculations were performed with the same normal pressures, frequency and amplitude of forced vibrations and drive velocity as assumed in the experimental tests. The values of the tangential stiffness coefficient, corresponding to the given values of normal pressures, were taken from the results of the conducted experimental tests (Fig. 5). Also, the value of the coefficient of friction $\mu = 0.193$ was determined experimentally for the tested sliding pair. The stiffness of the drive system k_d was 0.92e6 N/m.

Figure 8 presents a comparison of the results of experimental tests and numerical analyzes of the friction force reduction as a function of surface pressures od tested contact for four drive velocities v_d equal to 0.2, 0.5, 1 and 2 mm/s.

To assess the compatibility of the obtained numerical results with the results of experimental tests Root Mean Square Error (RMSE) was used, which value was calculated from the formula:

$$RMSE = \sqrt{\frac{1}{n}\sum_{i=1}^{n}\left(\bar{F}_{f_{E_i}} - \bar{F}_{f_{M_i}}\right)^2} \qquad (12)$$

where: $\bar{F}_{f_{E_i}}$ – average friction force determined from experiment,
$\bar{F}_{f_{M_i}}$ – average friction force determined from model,
n – number of experimental points.

The calculated Root Mean Squared Error values are summarized in Table 1.

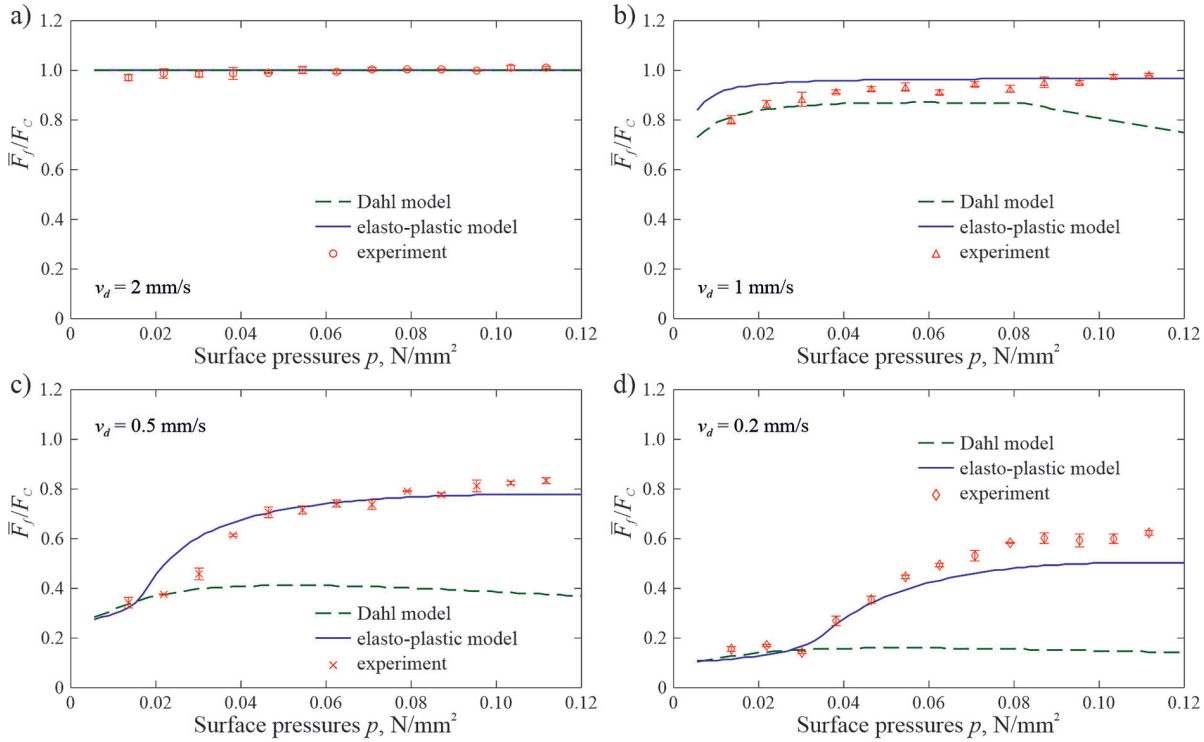

Fig. 8. Comparison of the results of experimental research and numerical calculations: a) v_d = 2 mm/s, b) v_d = 1 mm/s, c) v_d = 0.5 mm/s, d) v_d = 0.2 mm/s

The comparison of the results presented in Figure 8 and the list of the determined RMSE values given in Table 1 shows that for $v_a < v_d$ a significantly better compatibility of the numerical analysis results with the results of experimental tests is obtained for the elasto-plastic friction model then for the Dahl friction model. In the case of the Dahl model, good agreement with the experimental data is obtained only in the range up to p = 0.03 N/mm^2. Better compatibility of the elasto-plastic model at higher pressures results from the inclusion of the purely elastic deformation phase in the initial stage of the presliding displacement. When the drive velocity is greater than the vibration velocity amplitude, the calculation results of the friction force reduction using both models are the same – the friction force does not change, which means that in case, the longitudinal tangential vibrations have no effect on friction force.

CONCLUSIONS

Conducting reliable numerical analyzes with the use of dynamic friction models such as the Dahl model or the elasto-plastic model is impossible without knowing the value of the tangential contact stiffness coefficient k_t for the tested friction pair. The determination of the value of this coefficient for the analyzed steel-steel friction pair was one of the necessary conditions for the correct performance of simulation analyzes of the effect of normal pressures on the level of friction force reduction in the presence of longitudinal tangential vibrations presented in this paper.

Carried out experiments of the tangential stiffness clearly indicates that the increase in normal pressures causes an increase in the value of the tangential stiffness coefficient k_t. An increase in normal pressures may reduce the effectiveness of friction force reduction under the influence of forced longitudinal tangential vibrations. It is especially visible for cases where the drive velocity v_d is much lower than the vibration velocity amplitude v_a.

Table 1. RMSE values

Model	RMSE [N]			
	v_d = 0.2 mm/s	v_d = 0.5 mm/s	v_d = 1 mm/s	v_d = 2 mm/s
Dahl friction model	0.3286	0.3197	0.0982	0.0120
Elasto-plastic friction model	0.0743	0.0596	0.0533	0.0120

The friction model adopted for numerical analyzes has a significant impact on the calculated value of the friction force reduction caused by longitudinal tangential vibrations. The compatibility of the computational results with the experimental ones is strongly dependent on the applied surface pressures.

Acknowledgements

This research was funded in whole by National Science Centre, Poland; Grant No. 2021/05/X/ST8/01244. For the purpose of Open Access, the author has applied a CC-BY public copyright licence to any Author Accepted Manuscript (AAM) version arising from this submission.

REFERENCES

1. Gutowski P., Leus M.: Computational model of friction force reduction at arbitrary direction of tangential vibrations and its experimental verification. Tribology International 2020; 143: 106065.
2. Gutowski P., Leus M.: The effect of longitudinal tangential vibrations on friction and driving forces in sliding motion. Tribology International 2012; 55: 108–118.
3. Leus M., Abrahamowicz M. Experimental investigations of elimination the stick-slip phenomenon in the presence of longitudinal tangential vibration. Acta Mechanica et Automatica 2019; 13(1): 45–50.
4. Rybkiewicz M., Gutowski P., Leus M. Experimental and numerical analysis of stick-slip suppression with the use of longitudinal tangential vibration. Journal of Theoretical and Applied Mechanics 2020; 58(3): 637–648.
5. Rybkiewicz M., Leus M. Selection of the friction model for numerical analyses of the impact of longitudinal vibration on stick-slip movement. Advances in Science and Technology Research Journal 2021; 15(3): 277–287.
6. Gao H., De Volder M., Cheng T., Bao G., Reynaerts D. A pneumatic actuator based on vibration friction reduction with bending longitudinal vibration mode. Sensors and Actuators A: Physical 2016; 252: 112–119.
7. Kapelke S., Seemann W. On the effect of longitudinal vibrations on dry friction: Modelling aspects and experimental investigations. Tribology Letters 2018; 66(3): 1–11.
8. Littmann W., Stork H., Wallaschek J. Reduction of friction using piezoelectrically excited ultrasonic vibrations, Proceedings of the SPIE's 8th Annual International Symposium on Smart Structures and Material, Billingham, Washington 2001: 302–311.
9. Littmann W., Stork H., Wallaschek J. Sliding friction in the presence of ultrasonic oscillations: superposition of longitudinal oscillations. Archive of Applied Mechanics 2001; 71: 549–54.
10. Qu H., Zhou N., Guo W., Qu J. A model of friction reduction with in-plane high-frequency vibration. Proceedings of the Institution of Mechanical Engineers, Part J: Journal of Engineering Tribology 2016; 230(8): 962–967.
11. Storck H., Littmann W., Wallaschek J., Mracek M.: The effect of friction reduction in presence of ultrasonic vibrations and its relevance to traveling wave ultrasonic motors. Ultrasonic 2002; 40: 379–383.
12. Wang P., Ni H., Wang R., Li Z., Wang Y. Experimental investigation of the effect of in-plane vibrations on friction for different materials. Tribology International 2016; 99: 237–247.
13. Wang P., Ni H., Wang R., Liu W., Lu S. Research on the mechanism of in-plane vibration on friction reduction. Materials 2017; 10(9): 1–21.
14. Dahl P.R. A solid friction model. Technical Report TOR-158(3107–18), The Aerospace Corporation, El Segundo, CA, 1968.
15. Dahl P.R. Solid friction damping of mechanical vibrations. AIAA Journal 1976; 14(12): 1675–1682.
16. Dupont P., Armstrong B., Hayward V. Elasto-plastic friction model: contact compliance and stiction. Proceedings of the American Control Conference, Chicago, Illinois 2000, 1072–1077.
17. Dupont P., Hayward V., Armstrong B., Altpeter F. Single state elasto-plastic friction models. IEEE Transactions on Automatic Control 2002; 47(5): 787–792.
18. Burdekin M., Back N., Cowley A. Experimental study of normal and shear characteristics of machined surfaces in contact. Journal of Mechanical Engineering Scienc 1978; 20(3): 129–132.
19. Kirsanova V.N. Issliedovanie i rascet kasatelnoj podatlivosti ploskich stykov. Stanki i instrument 1967; 7: 22–24.
20. Koizumi T., Ito Y., Masuko M. Experimental expression of the tangential micro-displacement between joint surfaces. Bulletin of JSME 1979; 22(166): 591–597.
21. Leus M., Gutowski P. The experimental analysis of the tangential stiffness of the flat contact joints. Modelling in Engineering 2009; 6(37): 185–192.
22. Fu W.P., Huang Y.M., Zhang X.L. Experimental investigation of dynamic normal charac-teristics of machined joint surfaces. Journal of Vibration and Acoustics 2000; 122(4): 393–398.
23. Grudziński K., Kostek R. Influence of normal micro-vibrations in contact on sliding motion of solid body. Journal of Theoretical and Applied Mechanics 2005; 43(1): 37–49.
24. Leus M., Gutowski P. Theoretical and experimental analyses of the influence of normal vibrations on friction force in sliding motion. Tribologia 2014; 1: 53–62.
25. Grzejda R. FE-modelling of a contact layer between elements joined in preloaded bolted connections for the operational condition, Advances in Science and Technology Research Journal 2014; 8(24): 19–23.
26. Grzejda R. Study of the distribution of normal contact pressure between parts joined in a multi-bolted system under operational loads, Engineering Transactions 2019; 67(2): 147–155.
27. Bliman P.A. Mathematical study of the Dahl's friction model. European Journal of Mechanics, A/Solids 1992; 6: 835–848.